*Neuro-Oncology* 15(12):1664–1672, 2013.
doi:10.1093/neuonc/not112
Advance Access publication September 30, 2013



# Invasion patterns in brain metastases of solid cancers

Anna S. Berghoff, Orsolya Rajky, Frank Winkler, Rupert Bartsch, Julia Furtner, Johannes A. Hainfellner, Simon L. Goodman, Michael Weller, Jens Schittenhelm, and Matthias Preusser

*Institute of Neurology, Medical University of Vienna, Vienna, Austria (A.S.B., J.A.H.); Department of Medicine I, Medical University of Vienna, Vienna, Austria (O.R., R.B., M.P.); Comprehensive Cancer Center, CNS Unit (CCC-CNS), Vienna, Austria (A.S.B., O.R., R.B., J.A.H.); Neurology Clinic and National Center for Tumor Disease, University of Heidelberg, Heidelberg, Germany (F.W.); Department of Radiology, Medical University of Vienna, Vienna, Austria (J.F.); Therapeutic Area Oncology, Cellular Pharmacology, Merck-Serono, Darmstadt, Germany (S.L.G.); Department of Neurology, University Hospital Zurich, Zurich, Switzerland (M.W.); Department of Neuropathology, Institute of Pathology and Neuropathology, University of Tübingen, Tübingen, Germany (J.S.)*

**Background.** Brain metastases are generally considered to be well demarcated from the surrounding brain parenchyma, although infiltrative growth patterns have been observed. We systemically investigated infiltration patterns and expression of adhesion molecules in a large and well-defined series of autopsy cases of brain metastases.

**Methods.** Ninety-seven autopsy specimens from 57 brain metastasis patients (primary tumor: 27 lung cancer, 6 breast cancer, 8 melanoma, 2 colorectal cancer, 1 kidney cancer, and 13 other) were evaluated for patterns of invasion into surrounding brain parenchyma. Expression of integrins αv; cytoplasmic β3, αvβ3, αvβ5, αvβ6, and αvβ8; and of E and N cadherin were evaluated using immunohistochemistry.

**Results.** Three main invasion patterns were seen: well-demarcated growth (29/57, 51%), vascular co-option (10/57, 18%), and diffuse infiltration (18/57, 32%). There was no statistically significant association of invasion pattern with primary tumor type, although vascular co-option was most common in melanoma brain metastases (4/10). Invasion patterns of different brain metastases of the same patient were highly concordant ($P < .001$, chi-square test). Distance of infiltration from the main tumor mass ranged from 12.5 μm to 450 μm (median 56.2 μm) and was not significantly different between the vascular co-option and the diffuse infiltration groups. Levels of αvβ6 were significantly higher in the well-demarcated group than in the vascular co-option and the diffuse infiltration groups ($P = .033$, Kruskal-Wallis test). Expression of αvβ5 in tumor cells was higher in brain metastasis lesions previously treated with stereotactic radiosurgery ($P = .034$, chi-square test).

**Conclusions.** Distinct invasion patterns of brain metastases into the brain parenchyma are not specific for primary tumor types, seem to be influenced by expression of αv integrin complexes, and may help to guide clinical decision-making.

**Keywords:** adhesion molecules, brain metastases, cadherin, integrin, invasion.

Brain metastases are a frequent complication in oncology and affect up to 40% of patients with metastatic cancer.[1] While the incidence of brain metastases has shown a constant increase over the last decades, treatment options remain limited and rely mainly on local approaches like surgery, radiosurgery, or whole brain radiotherapy (WBRT).[2–4] Better understanding of the pathobiology of brain metastases may lead to novel treatments.

Brain metastases are usually regarded as growing in a well-delineated fashion within the brain parenchyma.[5] This notion is based mainly on their neuroradiological presentation with relatively sharp demarcation of contrast-enhancing areas and a generally better delineation than that of malignant gliomas. However, the histological patterns of invasion in brain metastases have so far not been addressed in comprehensive studies, although infiltrative behavior has occasionally been noted.[6,7] Clinically,

Received May 11, 2013; accepted June 17, 2013.

**Corresponding Author:** Matthias Preusser, MD, Department of Medicine I and Comprehensive Cancer Center, Central Nervous System Tumours Unit (CCC-CNS), Medical University of Vienna, Waehringer Guertel 18-20, 1090 Vienna, Austria (matthias.preusser@meduniwien.ac.at).

infiltrative behavior with unclear resection margins is regularly noted by neurosurgeons, and high local recurrence rates after surgery and radiosurgery have been reported for such cases.[8,9]

In general, cancer cells grow and invade solid tissues in different ways such as expansive growth, multicellular migration, and individual cell migration.[10] Migration and invasion require complex regulation of specific molecules, including adhesion molecules (eg, integrins, cadherins), cytoskeletal components (eg, actomyosin), proteolytic enzymes (eg, matrix metalloproteases [MMPs]), and others.[10–13] However, the types of invasive behavior of tumor cells have been described mostly in models of non-CNS tissues (eg, skin), and it is unknown whether similar mechanisms are active in the brain, with its distinct microenvironment. The CNS microenvironment differs from that of other solid organs. The brain parenchmya is composed of highly specialized cells (neurons, astrocytes, oligodendrocytes, microglia), and its extracellular matrix (ECM) has a distinct composition. It lacks constituents usually found in solid organs, such as fibronectin and collagen, but it is rich in proteoglycans, tenascin, laminin, heparin/chondroitin/dermatan sulfates, and hyaluronic acid.[14]

In this study we systemically characterized the invasion patterns of brain metastases and their correlation with the expression of several adhesion molecules in a series of autopsy specimens. Surgery specimens are not suitable for such studies, since in most cases they include no or only little well-preserved brain tissue around the resection margin and are thus not sufficient for investigation of the invasion front and the interaction of cancer cells with the brain parenchyma.

## Materials and Methods

### *Patients*

All patients with histologically proven brain metastases who underwent brain autopsy between 1987 and 2011 were identified from the Neuro-Biobank of the Medical University of Vienna. From each patient, at least one representative formalin-fixed and paraffin-embedded tissue block containing tumor tissue and surrounding brain parenchyma was selected. Clinical and demographic data were retrieved by chart review. This study was approved by the ethics committee of the Medical University of Vienna (ethics committee protocol number 078/2004).

### *Evaluation of Invasion Patterns*

Evaluation of invasion patterns was performed on one routinely stained hematoxylin and eosin (H&E) section per tumor block. For enhanced visibility and better evaluation of single tumor cells, immunohistochemistry for cytokeratin (carcinomas) or HMGB45 (melanomas) and for evaluation of vascular structure immunohistochemistry for CD34 was performed on an automated horizontal slide-processing system (AutostainerPlusLink, Dako) using standard protocols in selected cases (Table 1).[15–17] Maximal invasion distance of tumor cells from the main tumor mass was microscopically measured on H&E slides with a grid of 25 μm length at 400× magnification.

### *Immunohistochemistry and Evaluation of Integrins and Cadherins*

Immunohistochemistry for the αv subunit, cytoplasmic β3, and αvβ3, αvβ5, αvβ6, and αvβ8 complexes was performed with a fully automated multimodal slide-staining system (BenchMark, Ventana Medical Systems) as described previously.[18] In brief, an indirect biotin-avidin system with standard cell conditioner 1 and EDTA pretreatment protocol were used. Signal amplification was achieved with a copper enhancer (iView DAB Detection Kit, Ventana Medical Systems).[19] Immunohistochemistry for E cadherin and N cadherin was performed using an automated horizontal slide-processing system (AutostainerPlusLink, Dako). In brief, antigen retrieval was performed with ph9 buffer (Flex TRS high, Dako). Slides were incubated with primary antibody for 1 h for N cadherin (anti–N cadherin antibody, ab18203, solution 1:500, abcam) and overnight for E

**Table 1.** Antibodies

| Antibody to | Clone | Dilution | Positive Control | Source |
|---|---|---|---|---|
| αv subunit | EM01309 | 1:1000* | HT29 colon cancer cell line, DU-145 prostate cancer cell line | Goodman et al[18] |
| β3 subunit | EM00212 | 1:500* | Normal kidney, malignant melanoma | Goodman et al[18] |
| αvβ3 | EM22703 | 1:500 | Normal kidney, malignant melanoma | Goodman et al[18] |
| αvβ5 | EM09902 | 1:800* | Normal colon tissue, HT29 colon cancer cell line | Goodman et al[18] |
| αvβ6 | EM05201 | 1:1000* | Normal kidney, HT29 colon cancer cell line | Goodman et al[18] |
| αvβ8 | EM13309 | 1:1000* | Normal peripheral nerve, Ovcar-3 ovarian cancer cell line | Goodman et al[18] |
| E cadherin | Ab15148 | 1:30 | Skin | Abcam |
| N cadherin | Ab18203 | 1:500 | Liver carcinoma | Abcam |
| CD34 | NCL-END | 1:500 | Glioblastoma | Novocastra, |
| Pan-cytokeratin | Lu5 | 1:100 | Lung carcinoma | BMA Biomedicals |
| HMBG45 | HMB45 | 1:50 | Melanoma | Dako |

*Protein concentration 1 mg/mL.

cadherin (anti–E cadherin antibody, ab15148, solution 1:30, abcam). Adequate positive and negative controls were included in each run. Table 1 lists antibodies, clones, dilution, positive controls, and sources of reagents.

Analyses of immunohistochemical staining of the integrin αv subunit, cytoplasmic β3, αvβ3, αvβ5, αvβ6, and αvβ8 complexes, and E cadherin and N cadherin were performed by calculating the H-score.[20,21] In brief, the intensity of membranous staining was multiplied by the percentage of cells showing a specific, complete, membranous immunoreactivity. Further, integrin and cadherin expression of the vascular structures of the surrounding brain parenchyma, tumor vessels, peritumoral vessel, and stroma was evaluated semiquantitatively and recorded as either positive or negative.

### *Macroscopic Autopsy and Radiology*

For illustrative purposes, we retrospectively retrieved digitized photographs of the macroscopic autopsy specimens and premortem cranial MR images of the investigated patient cohort from the archives of our Neuro-Biobank and the Department of Neuroradiology where available.

### *Statistics*

We performed exploratory analyses of the correlation between invasion pattern and integrin and cadherin expression. For correlation of 2 binary variables, the chi-square test was used. For correlation of medians between invasion groups, the Kruskal–Wallis test was performed. For correlation of invasion patterns with time from first diagnosis of brain metastases to death (overall survival time), we used the Kaplan–Meier method and the log-rank test. Patients in whom brain metastases were detected at death were excluded from survival analysis. As the purpose of the study was exploratory, no adjustment for multiple testing was applied.[22] All statistics were calculated using Statistical Package for the Social Sciences 20.0 software.

## Results

### *Patients' Characteristics*

Fifty-seven patients (26 female, 31 male) with a median age of 58 years (range 27–91) at death were included in the analysis. Overall, 97 autopsy specimens were evaluated. Available for investigation were 1 brain metastasis tissue block in all 57 patients, 2 distinct brain metastasis tissue blocks in 30/57 (52.6%) patients, and 3 distinct brain metastasis tissue blocks in 10/57 (17.5%) patients. In 18/57 (31.6%) patients, diagnosis of brain metastases was made only at autopsy. Twenty-three of 57 (40.4%) patients received treatment for brain metastases. First-line treatment for brain metastases was surgery in 7/57 (12.3%) patients, stereotactic radiosurgery (SRS) in 8/57 (14.0%), WBRT in 4/57 (7.0%), and chemotherapy in 4/57 (7.0%). Overall, 7/57 (12.3%) patients received WBRT during the course of disease, 7/57 (12.3%) received SRS of the brain metastasis investigated in this study, and 17/57 (29.8%) patients received chemotherapy during the course of disease. Upon diagnosis of brain metastases, 34/57 (59.6%) patients were treated with best supportive care. According to autopsy protocols, brain metastases were the cause of death in 19/57 (33.3%) patients. Table 2 summarizes further the patients' characteristics, and detailed compilation is given in Supplemental Table S1.

### *Invasion Patterns of Brain Metastases*

***Histomorphology.***—We delineated 3 distinct invasion patterns: 29/57 (50.9%) brain metastases showed a distinct, well-demarcated border to the surrounding brain parenchyma (well-demarcated group); 10/57 (17.5%; Fig. 1A) brain metastases showed distinct perivascular protrusions of multicellular tumor cell formations from the main tumor mass into the brain parenchyma (vascular co-option group; Fig. 1B); and 18/57 (31.6%) brain metastases showed a diffuse infiltration of single tumor cells into the surrounding brain parenchyma (diffuse infiltration group; Fig. 1C). Generally, the invasion pattern was consistent throughout major parts (>90% of the border) of the tumor/brain border in individual metastases.

In 30/57 (52.6%) cases, multiple distinct brain metastases of the same patient were available for investigation, and the invasion type was generally highly congruent among the lesions ($P < .001$, chi-square test; Table 3).

Median maximal measurable invasion distance of tumor cells from the border of the main tumor mass was 68.7 μm (range 12.5–125 μm) in the vascular co-option group and 56.2 μm (range 12.5–450 μm) in the diffuse infiltration group. The maximal measurable invasion distance was not different between the vascular co-option group and the diffuse infiltration group ($P = .486$, *t*-test).

***Correlation with primary tumor type.***—Brain metastases of melanoma tended to grow via vascular co-option more often than other primary tumors (4/8). The most frequent primary tumor in the well-demarcated as well as in the diffuse infiltration group was lung cancer. Brain metastases of small cell lung cancer (SCLC) showed frequently a diffuse infiltrative growth (2/3), whereas non-SCLC (NSCLC) grew rather well demarcated (13/24, 54.2%). Squamous NSCLC was more common in the well-demarcated group (4/6), whereas adenocarcinoma NSCLC was equally represented in the well-demarcated (5/12, 41.7%) and the diffuse infiltration group (5/12, 41.7%). See Table 2 for correlation of invasion patterns with primary tumor type.

***Correlation with treatment.***—Complete information on applied therapies after diagnosis of brain metastases was available for 55/57 (96.5%) patients. No statistically significant association was observed between first-line or other brain metastasis treatment and invasion patterns (Table 2). In the diffuse infiltration group, a higher proportion of patients had received WBRT at any time

**Table 2.** Patient characteristics and integrin expression

| Characteristic | Well-demarcated ($n = 29$) | | Vascular Co-option ($n = 10$) | | Diffuse Infiltration ($n = 18$) | | Chi-square Test, Kruskal–Wallis Test |
|---|---|---|---|---|---|---|---|
| | *n* | % | *n* | % | *n* | % | |
| Primary tumor type | | | | | | | |
| Lung Cancer | 14 | 51.9 | 3 | 11.1 | 10 | 37.0 | |
| NSCLC | 13 | 54.2 | 3 | 12.5 | 8 | 33.3 | |
| AdenoCa | 5 | 41.7 | 2 | 16.7 | 5 | 41.7 | |
| SquamousCa | 4 | 66.7 | 0 | 0 | 2 | 33.3 | |
| Large cell Ca | 2 | 100.0 | 0 | 0 | 0 | 0 | |
| Not otherwise specified | 2 | 50.0 | 1 | 25.0 | 1 | 25.0 | |
| SCLC | 1 | 33.3 | 0 | 0.0 | 2 | 66.7 | 0.285 |
| Breast Cancer | 3 | 50.0 | 0 | 0.0 | 3 | 50.0 | |
| Melanoma | 2 | 25.0 | 4 | 50.0 | 2 | 25.0 | |
| Kidney Cancer | 1 | 100.0 | 0 | 0.0 | 0 | 0.0 | |
| Colorectal Cancer | 2 | 100.0 | 0 | 0.0 | 0 | 0.0 | |
| Other | 7 | 53.8 | 3 | 23.1 | 3 | 23.1 | |
| Localization of investigated brain metastasis | | | | | | | |
| Supratentorial | 22 | 47.8 | 8 | 17.4 | 16 | 34.8 | 0.545 |
| Infratentorial | 7 | 63.6 | 2 | 18.2 | 2 | 18.2 | |
| Treatment of investigated brain metastasis | | | | | | | |
| Gamma Knife | | | | | | | 0.334 |
| Yes | 5 | 71.4 | 0 | 0.0 | 2 | 28.6 | |
| No | 23 | 46.9 | 10 | 20.4 | 16 | 32.7 | |
| WBRT | | | | | | | 0.309 |
| Yes | 2 | 28.6 | 1 | 14.3 | 4 | 57.1 | |
| No | 26 | 53.1 | 9 | 18.4 | 14 | 28.6 | |

point (4/18; 22%) compared with the well-demarcated group (2/28, 7.1%) or the vascular co-option group (1/10). Further, a higher proportion of patients had received chemotherapy during their course of disease in the diffuse infiltration group (8/17, 47.1%) than in the well-demarcated (8/28, 28.6%) or the vascular co-option group (1/10).

***Correlation with clinical characteristics.***—Survival times from first diagnosis of brain metastases were available in 37 patients. Median survival from diagnosis of brain metastases was 2.0 months in the well-demarcated group ($n = 19$), 1.8 months in the vascular co-option group ($n = 5$), and 1.8 months in the diffuse infiltration group ($n = 13$). There was no statistically significant correlation of invasion pattern with survival time from diagnosis of brain metastases in this small cohort ($P = .945$, log-rank test). Patients in the well-demarcated group had more often a singular brain metastasis at first diagnosis of brain metastases (52%) than the vascular co-option (33.3%) or diffuse infiltration group (35.7%; $P = .483$, chi-square test). Extracranial metastases were present in 19/57 (33.3%) patients. No difference in the presence of extracranial metastases was observed between the 3 invasion patterns ($P = .781$, chi-square test). In the cohort of all 56 patients, there was no significant association of invasion pattern with survival time ($P = .825$, log-rank test).

***Correlation with macroscopic pathology findings and neuroradiology.***—Illustrative correlations of macroscopic pathology and neuroradiological findings with histological invasion patterns are shown in Fig. 1. The low number of available macroscopic photographs ($n = 4$) and premortal neuroradiological images ($n = 5$) precluded systematic correlation with histological findings.

### *Integrin Expression*

***General description.***—Alpha-v integrins showed strong membranous expression on tumor, vascular, and stromal cells in variable fractions of cases. In general, the majority of specimens showed homogeneous αv integrin expression patterns throughout the tumor tissue, except for αvβ8 expression, which was absent in the majority of specimens (Supplemental Table S1). However, regional accentuation of integrin expression was observed in some specimens. Accentuated expression in perivascular tumor cells was observed in 11/57 (19.3%), 9/57 (15.8%), and 4/57 (7.0%) cases for the αv subunit, αvβ6, and αvβ5, respectively. Perinecrotic overexpression of αvβ6, αv subunit, and αvβ5 was found in 4/57 (7.0%), 2/57 (3.5%), and 2/57 (3.5%) cases, respectively (Fig. 2).

Analyzing expression on vascular structures, we observed αvβ5 integrin expression on all (57/57, 100%)

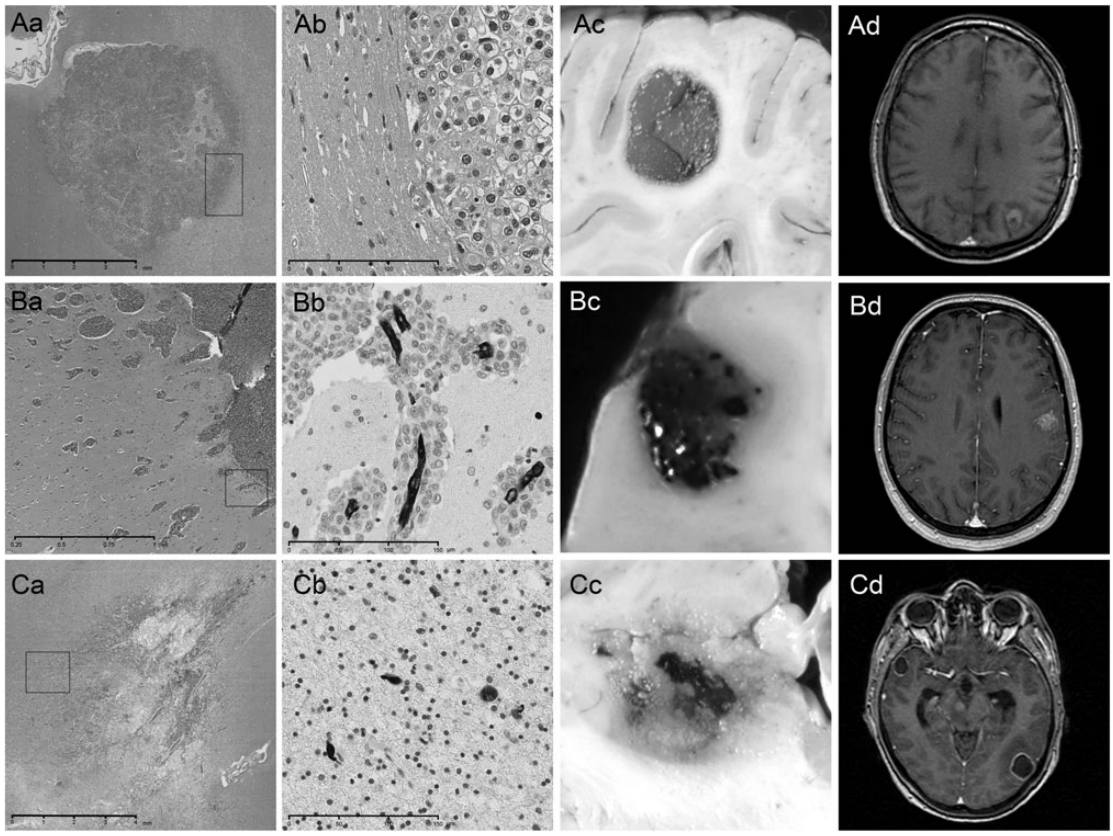


Fig. 1. Distinct invasion patterns in human brain metastases. Top row: example of well-demarcated invasion (patient 5, NSCLC, Supplemental Table S1): (Aa) H&E slide (magnification ×1.25); (Ab) invasion front of well-demarcated brain metastasis (magnification × 400); (Ac) macroscopic sample of well-demarcated brain metastasis; (Ad) MRI contrast-enhanced T1-weighted sequence sample of well-demarcated brain metastasis. Middle row: example of vascular co-option (patient 13, melanoma, Supplemental Table S1): (Ba) H&E slide (magnification × 1.25); (Bb) CD34 immunohistochemistry of vascular co-option (magnification × 400); (Bc) macroscopic sample of brain metastasis growing via vascular co-option; (Bd) MRI contrast-enhanced T1-weighted sequence sample of brain metastasis growing via vascular co-option. Bottom row: example of diffuse invasion (patient 2, SCLC, Supplemental Table S1): (Ca) H&E of brain metastasis (magnification × 1.25); (Cb) CD18 cytokeratin staining showing diffusely infiltrating tumor cells; (Cc) macroscopic sample of diffuse infiltrating brain metastasis; (Cd) MRI contrast-enhanced T1-weighted sequence sample of diffuse infiltrating brain metastasis. Color figures available from authors upon request.

**Table 3.** Concordance between first, second, and third brain metastases

| First Brain Metastasis ($n = 57$) | Well-demarcated ($n = 29$) | | Vascular Co-option ($n = 10$) | | Diffuse Infiltration ($n = 18$) | | Chi-square Test |
|---|---|---|---|---|---|---|---|
| | *n* | % | *n* | % | *n* | % | |
| Second brain metastasis ($n = 30$) | | | | | | | |
| Well-demarcated | 14 | 100 | 0 | 0 | 0 | 0 | |
| Vascular co-option | 1 | 17 | 5 | 80 | 0 | 0 | $P < .001$ |
| Diffuse infiltration | 0 | 0 | 1 | 10 | 9 | 90 | |
| Third brain metastasis ($n = 10$) | | | | | | | |
| Well-demarcated | 3 | 60 | 1 | 20 | 1 | 20 | |
| Vascular co-option | 0 | 0 | 3 | 100 | 0 | 0 | $P = .023$ |
| Diffuse infiltration | 0 | 0 | 0 | 0 | 2 | 100 | |

vessels, including tumoral and peritumoral vessels as well as the vascular structures of the surrounding brain parenchyma. Alpha-vβ3 expression was not observed on the vascular structures of the surrounding brain parenchyma, except randomly on some larger vessels of the meninges. Prominent expression of αvβ3 was observed on angiogenic, sprouting vessels with multilayered endothelium within the tumor and in the peritumoral area. In 30/57

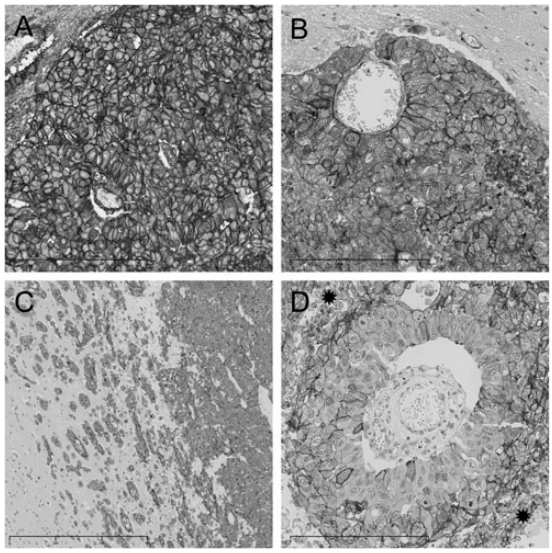


Fig. 2. Integrin expression patterns: (A) αv subunit expression (patient 5, NSCLC, Supplemental Table S1); (B) αvβ5 expression with accentuation around a vessel (patient 5, NSCLC, Supplemental Table S1); (C) αvβ5 expression in a brain metastasis growing via vascular co-option (patient 13, melanoma, Supplemental Table S1); (D) αvβ6 expression with accentuation around necrosis, the stars at upper left and lower right mark the necrosis (patient 5, NSCLC, Supplemental Table S1). Color figures available from authors upon request.

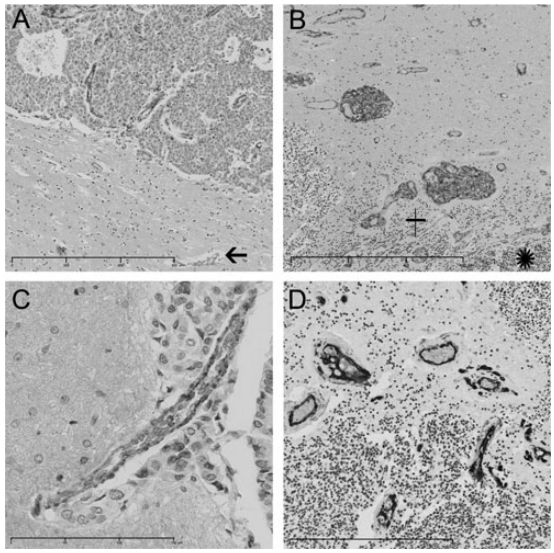


Fig. 3. Integrin expression in vascular structures: (A) αvβ3 expression on tumor vessel, arrow marks a vessel in the peritumoral area without αvβ3 expression (patient 5, NSCLC, Supplemental Table S1); (B) αvβ3 expression in glomeruloid-like vessels of the peritumoral area, the star at lower right marks the tumor tissue, the cross marks the surrounding cerebellum (patient 8, SCLC, Supplemental Table S1); (C) αvβ3 expression in a vessel with vascular co-option (patient 13, melanoma, Supplemental Table S1); (D) CD34 immunohistochemistry of the case shown in (B), illustrating the peritumoral sprouting vessels (patient 8, SCLC, Supplemental Table S1). Color figures available from authors upon request.

(52.6%) specimens, immunoreactivity for αvβ3 of the angiogenic tumor vessels was observed, and in 29/57 (50.9%) specimens, angiogenic vessels in the peritumoral area showed specific immunoreactivity for αvβ3. Specific immunoreactivity for the β3 subunit was observed in angiogenic tumor vessels of 46/57 (80.7%) specimens and in angiogenic vessels in the peritumoral area of 45/57 (78.9%) specimens (Fig. 3). The expression detected for the αvβ3 complex was generally lower than for the β3 cytoplasmic domain. The β3 chain is on 2 integrin complexes, αvβ3 and glycoprotein IIbIIIa (the platelet fibrinogen receptor). Tissue localization suggested that the staining of β3 was not due to platelet deposits or aggregates. The αvβ3 antibody used (EM22703) preferentially binds particular ligated conformation of αvβ3, while the cytoplasmic-β3 antibody (EM00212) does not discriminate.[18] This may explain the difference in staining results between these antibodies.

Fibrous tumoral stroma was observed in 32/57 (56.1%) specimens and showed expression of the αv subunit (32/32, 100%), αvβ3 (2/32, 6.3%), αvβ5 (28/32, 87.5%), and αvβ6 (6/32, 18.8%).

Relative overexpression of αv integrins at the invasion front was not consistently found, but only in some specimens (αv subunit: 8/57, 14.0%; αvβ5: 8/57, 14.0%; αvβ6: 8/57, 14.0%).

***Correlation with invasion patterns.***—Median H-score of αvβ6 was significantly higher in the well-demarcated group (median 90, range 0–300) than in the vascular co-option group (median 0, range 0–120) and the diffuse infiltration group (median 30, range 0–120; $P = .033$, Kruskal–Wallis test). No correlation of invasion pattern and median H-score of αv subunit, αvβ3, αvβ5, αvβ8, or β3 subunit was observed.

***Correlation with therapy.***—Brain metastases previously treated with SRS presented more frequently with αvβ5 expression in the tumor cells (6/7) than did specimens without prior SRS (21/49, 42.9%; $P = .034$, chi-square test). Furthermore, the median αvβ5 H-score was significantly higher in brain metastases with prior SRS (60 vs 0; $P = .05$, Mann–Whitney *U*-test). No correlation between SRS treatments and αv subunit, αvβ3, αvβ6, αvβ8, or β3 subunit expression was observed. Prior WBRT or chemotherapy did not show a significant correlation with expression of any of the integrin subunits investigated in this study.

### *Cadherin Expression*

Of the tumor specimens studied, 42/57 (73.7%) showed expression of E cadherin, 10/57 (17.5%) showed expression of N cadherin, and 6/57 (10.5%) showed expression of both cadherins. No significant correlation of median H-score of E cadherin or N cadherin and invasion pattern or primary tumor types was observed. Nine of 57 (15.8%) specimens showed increased E cadherin expression at the invasion front. Three of 57 (5.3%)

specimens showed overlapping increased expression at the invasion front of E cadherin and αv, 2/57 (3.5%) showed overlapping expression with αvβ5, and 1/57 (1.8%) specimen showed overlapping expression with αvβ6 at the invasion front. No cadherin expression was observed in the tumor stroma or vascular structures.

## Discussion

Brain metastases are an increasing challenge in oncological practice, as survival in many types of solid cancers is increased by novel treatment strategies. The dominant treatment strategies for brain metastases are local and include surgery and radiosurgery. The benefit from local treatments is likely to be heavily affected by the degree to which macroscopically focal disease is truly focal on a microscopic level. Accordingly, the brain metastasis/brain interface may assume major prognostic significance.

Here, we delineate 3 distinct invasion patterns of brain metastases: well-demarcated growth, vascular co-option, and diffuse infiltration. We found a high fraction of cases showing invasive growth via vascular co-option (18%) or single-cell infiltration (32%). These surprising findings challenge the general notion that brain metastases predominantly grow in an expansive and well-delineated fashion, but they are in good agreement with previous results from experimental studies, smaller and less comprehensive investigations on human tissue samples, and clinical observations.

In half of our cases, we observed expansive growth of an outwardly extending tumor mass within the brain parenchyma. Expression levels of αvβ6 were significantly higher in this group of well-demarcated tumors. Integrin αvβ6 is not expressed in healthy adult epithelia but is upregulated in cancer and has been shown to modulate invasion and inhibit apoptosis.[23] However, the exact role of αvβ6 in cancer pathobiology and in particular in brain metastases remains to be determined.

The vascular basement membrane may act as a guiding track for perivascular growth of cell collectives. Our results indicate that this invasion behavior is not only present in mesenchymal and epithelial tissues but also occurs in the distinct microenvironment of the CNS. In line with previous studies, we observed vascular co-option most commonly in melanoma brain metastases; however, we found it also in other tumor types, such as NSCLC adenocarcinoma.[24–26]

Single-cell infiltration into the brain parenchyma of brain-metastatic tumor cells has previously been reported to be characteristic for SCLC.[7] Our data show that this invasion pattern is also not uncommon in brain metastases of other tumor types, including NSCLC adenocarcinoma/squamous cell carcinoma, breast cancer, and melanoma. The high fraction of brain metastasis cases showing infiltrative growth has implications for local therapy options and highlights the need for including a safety margin beyond the neuroradiologically visible tumor borders.[6] In our study, depth of invasion into the CNS parenchyma from the main tumor mass reached up to 450 μm. Of note, SRS uses no margins for treatment, but at 0.4 mm from the prescription isodose line, nearly a full dose is delivered, and therefore the magnitude of invasion has no clear consequence on SRS practice. The selection of patients in need of an extended local treatment approach is challenging, as the current neuroradiological techniques cannot precisely visualize the invasion distance of a given tumor. However, we previously demonstrated that the extent of peritumoral brain edema might function as a surrogate marker for infiltrative tumor growth, as little brain edema was significantly more common in infiltrative brain metastases and correlated with impaired patient survival times.[8] Further prospective studies need to address the prognostic implications of brain metastasis invasion patterns in more detail.

We did not observe a statistically significant correlation of treatment modality with invasion pattern in our cohort. However, a higher proportion of patients in the diffuse infiltration group had received prior radiation or chemotherapy. As our sample size is not adequate for firm statistical conclusions, we cannot exclude that radio- or chemotherapy may select for or produce tumor cells with a higher infiltrative potential, similarly to some observations in primary tumors and gliomas.[27] Interestingly, brain metastasis lesions previously treated with SRS showed higher expression of αvβ5, a finding that is well in line with previous reports showing that this molecule is essential for tumor growth in preirradiated stroma.[28] Further, we observed a high consistency of invasion behavior between the growth patterns of different brain metastases in individual patients. This again may indicate that intrinsic molecular features of metastases originating from a given primary tumor correlate with certain invasion patterns.

Our results have to be interpreted with caution because the small sample sizes often do not allow firm statistical conclusions. Herein, we concentrated on the descriptive presentation of our results. However, it has to be taken into account that autopsy samples of brain metastases are very rare, and our series displays a rather large cohort compared with previously published studies on autopsy specimens.[6,7]

We noted prominent expression of αv integrins in many brain metastasis cases. This underscores the important function of this class of molecules in metastatic cancer. Currently, several integrin inhibitors are under clinical development, and promising activity was shown in some of the most frequent primary tumors of brain metastases such as NSCLC and melanoma.[29–31] Interestingly, the anti–αv-integrin antibody intetumumab reduced brain metastasis outgrowth in mice after intracarotid infusion of brain-seeking human epidermal growth factor receptor 2–positive breast cancer cells.[32] Thus, clinical trials specifically investigating the potential of integrin inhibitors for prophylaxis and treatment of brain metastases seem warranted.

## Supplementary Material

Supplementary material is available online at *Neuro-Oncology* (http://neuro-oncology.oxfordjournals.org/).

## Acknowledgments

We thank Irene Leisser and Gerda Ricken for excellent technical assistance with preparation of tissue specimens. Further we thank Prof Dr Harald Heinzl (Center for Medical Statistics, Informatics, and Intelligent Systems, Medical University of Vienna) for the supervision and advice with statistical analyses. This study was performed within the PhD thesis project of Anna Sophie Berghoff in the PhD program "Clinical Neuroscience (CLINS)" at the Medical University Vienna.

## Funding

The costs for this project were covered by the research budget of the Medical University of Vienna and the University of Tübingen.

*Conflict of interest statement*. S.L.G. is an employee at Merck-Serono and has a patent application referring to the anti-integrin antibodies used here. M.W. has received research support and honoraria for lectures and service on its advisory board from Merck-Serono. All other authors declare no conflict of interest.

## References

1. Gavrilovic IT, Posner JB. Brain metastases: epidemiology and pathophysiology. *J Neurooncol*. 2005;75(1):5–14.
2. Gaspar LE, Mehta MP, Patchell RA, et al. The role of whole brain radiation therapy in the management of newly diagnosed brain metastases: a systematic review and evidence-based clinical practice guideline. *J Neurooncol*. 2010;96(1):17–32.
3. Kalkanis SN, Kondziolka D, Gaspar LE, et al. The role of surgical resection in the management of newly diagnosed brain metastases: a systematic review and evidence-based clinical practice guideline. *J Neurooncol*. 2010;96(1):33–43.
4. Linskey ME, Andrews DW, Asher AL, et al. The role of stereotactic radiosurgery in the management of patients with newly diagnosed brain metastases: a systematic review and evidence-based clinical practice guideline. *J Neurooncol*. 2010;96(1):45–68.
5. Wesseling P, von Deimling A, Aldape K. Metastatic Tumours of the CNS. 4th ed. Lyons, France: IARC Press; 2007.
6. Baumert BG, Rutten I, Dehing-Oberije C, et al. A pathology-based substrate for target definition in radiosurgery of brain metastases. *Int J Radiat Oncol Biol Phys*. 2006;66(1):187–194.
7. Neves S, Mazal PR, Wanschitz J, et al. Pseudogliomatous growth pattern of anaplastic small cell carcinomas metastatic to the brain. *Clin Neuropathol*. 2001;20(1):38–42.
8. Spanberger T, Berghoff AS, Dinhof C, et al. Extent of peritumoral brain edema correlates with prognosis, tumoral growth pattern, HIF1a expression and angiogenic activity in patients with single brain metastases. *Clin Exp Metastasis*. 2013;30(4):357–368.
9. McPherson CM, Suki D, Feiz-Erfan I, et al. Adjuvant whole-brain radiation therapy after surgical resection of single brain metastases. *Neuro Oncol*. 2010;12(7):711–719.
10. Friedl P, Alexander S. Cancer invasion and the microenvironment: plasticity and reciprocity. *Cell*. 2011;147(5):992–1009.
11. Desgrosellier JS, Cheresh DA. Integrins in cancer: biological implications and therapeutic opportunities. *Nat Rev Cancer*. 2010;10(1):9–22.
12. Guo W, Giancotti FG. Integrin signalling during tumour progression. *Nat Rev Mol Cell Biol*. 2004;5(10):816–826.
13. Hood JD, Cheresh DA. Role of integrins in cell invasion and migration. *Nat Rev Cancer*. 2002;2(2):91–100.
14. Bonneh-Barkay D, Wiley CA. Brain extracellular matrix in neurodegeneration. *Brain Pathol*. 2009;19(4):573–585.
15. Mazal PR, Czech T, Sedivy R, et al. Prognostic relevance of intracytoplasmic cytokeratin pattern, hormone expression profile, and cell proliferation in pituitary adenomas of akromegalic patients. *Clin Neuropathol*. 2001;20(4):163–171.
16. Gelpi E, Popovic M, Preusser M, Budka H, Hainfellner J. Pleomorphic xanthoastrocytoma with anaplastic features presenting without GFAP immunoreactivity: implications for differential diagnosis. *Neuropathology*. 2005;25(3):241–246.
17. Birner P, Piribauer M, Fischer I, et al. Vascular patterns in glioblastoma influence clinical outcome and associate with variable expression of angiogenic proteins: evidence for distinct angiogenic subtypes. *Brain Pathol*. 2003;13(2):133–143.
18. Goodman SL, Grote HJ, Wilm C. Matched rabbit monoclonal antibodies against alphav-series integrins reveal a novel alphavbeta3-LIBS epitope, and permit routine staining of archival paraffin samples of human tumors. *Biol Open*. 2012;1(4):329–340.
19. Schittenhelm J, Schwab EI, Sperveslage J, et al. Longitudinal Expression analysis of alphav integrins in human gliomas reveals upregulation of integrin alphavbeta3 as a negative prognostic factor. *J Neuropathol Exp Neurol*. 2013;72(3):194–210.
20. Cappuzzo F, Hirsch FR, Rossi E, et al. Epidermal growth factor receptor gene and protein and gefitinib sensitivity in non-small-cell lung cancer. *J Natl Cancer Inst*. 2005;97(9):643–655.
21. Hirsch FR, Varella-Garcia M, Bunn PA, Jr., et al., Epidermal growth factor receptor in non-small-cell lung carcinomas: correlation between gene copy number and protein expression and impact on prognosis. *J Clin Oncol*. 2003;21(20):3798–3807.
22. Bender R, Lange S. Adjusting for multiple testing—when and how? *J Clin Epidemiol*. 2001;54(4):343–349.
23. Bandyopadhyay A, Raghavan S. Defining the role of integrin alphavbeta6 in cancer. *Curr Drug Targets*. 2009;10(7):645–652.
24. Kienast Y, von Baumgarten L, Fuhrmann M, et al. Real-time imaging reveals the single steps of brain metastasis formation. *Nat Med*. 2010;16(1):116–122.
25. Dome B, Paku S, Somlai B, Timar J. Vascularization of cutaneous melanoma involves vessel co-option and has clinical significance. *J Pathol*. 2002;197(3):355–362.
26. Leenders WP, Kusters B, Verrijp K, et al. Antiangiogenic therapy of cerebral melanoma metastases results in sustained tumor progression via vessel co-option. *Clin Cancer Res*. 2004;10(18 Pt 1):6222–6230.
27. Wild-Bode C, Weller M, Rimner A, Dichgans J, Wick W. Sublethal irradiation promotes migration and invasiveness of glioma cells: implications for radiotherapy of human glioblastoma. *Cancer Res*. 2001; 61(6):2744–2750.
28. Monnier Y, Farmer P, Bieler G, et al. CYR61 and alphaVbeta5 integrin cooperate to promote invasion and metastasis of tumors growing in preirradiated stroma. *Cancer Res*. 2008;68(18):7323–7331.

29. Goodman SL, Picard M. Integrins as therapeutic targets. *Trends Pharmacol Sci*. 2012;33(7):405–412.
30. Manegold C, Vansteenkiste J, Cardenal F, et al. Randomized phase II study of three doses of the integrin inhibitor cilengitide versus docetaxel as second-line treatment for patients with advanced non-small-cell lung cancer. *Invest New Drugs*. 2013;31(1): 175–182.
31. O'Day S, Pavlick A, Loquai C, et al. A randomised, phase II study of intetumumab, an anti-alphav-integrin mAb, alone and with dacarbazine in stage IV melanoma. *Br J Cancer*. 2011;105(3):346–352.
32. Wu YJ, Muldoon LL, Gahramanov S, Kraemer DF, Marshall DJ, Neuwelt EA. Targeting alphaV-integrins decreased metastasis and increased survival in a nude rat breast cancer brain metastasis model. *J Neurooncol*. 2012;110(1):27–36.